RESEARCH ARTICLE

Involvement of aquaporins in a mouse model of rotavirus diarrhea

Meiwan Cao[1], Min Yang[1], Zhiying Ou[1], Dingyou Li[2], Lanlan Geng[1], Peiyu Chen[1], Huan Chen[1], Sitang Gong[1✉]

1. Department of Gastroenterology, Guangzhou Women and Children's Medical Center, Guangzhou 510623, China
2. Department of Gastroenterology, Children's Mercy Hospital, University of Missouri Kansas City School of Medicine, 2401 Gillham Road, Kansas 64108, USA

Rotavirus diarrhea is a major worldwide cause of infantile gastroenteritis; however, the mechanism responsible for intestinal fluid loss remains unclear. Water transfer across the intestinal epithelial membrane seems to occur because of aquaporins (AQPs). Accumulating evidence indicates that alterations in AQPs may play an important role in pathogenesis. Here, we focus on changes in AQPs in a mouse model of rotavirus diarrhea. In the present study, 32 of 35 mice developed diarrhea and mild dehydration within 24 hours after infection with rotavirus strain SA11. Intestinal epithelial cells demonstrated cytoplasmic vacuolation, malaligned villi, and atrophy. AQP1 expression was significantly attenuated in the ileum and colon in comparison with controls; likewise, AQP4 and -8 protein expression were significantly decreased in the colon of rotavirus diarrhea-infected mice. In contrast, AQP3 protein expression was significantly increased in the colon of rotavirus-infected mice in comparison with controls. These results indicate that rotavirus diarrhea is associated with the downregulation of AQP1, -4, and -8 expression. Therefore, AQPs play an important role in rotavirus diarrhea.

KEYWORDS rotavirus; aquaporin; AQP; diarrhea; mice; intestine

INTRODUCTION

Worldwide, rotavirus is the leading cause of severe diarrhea in infants and young children between 6 months and 2 years of age, resulting in high mortality and morbidity. An estimated 527,000 children < 5 years of age die from rotavirus diarrhea each year, and > 85% of these deaths occur in low-income countries in Africa and Asia (CDC, 2008). Despite extensive studies in different animal models, the pathogenesis of rotavirus-induced diarrhea remains poorly understood. Various mechanisms have been proposed to explain rotavirus-induced diarrhea, including the decrease in the absorptive surface area due to short villi, decreased disaccharidase activity

resulting in the malabsorption of carbohydrates, disruption of the tight junctions in the small intestines, and altered ion channel transport due to the secretion of neurotransmitters such as 5-hydroxytryptamine (5-HT) and Vasoactive intestinal peptide (VIP) (Guttman J A, et al., 2007; Hodges K, et al., 2010).

Aquaporins (AQPs) are water-channel membrane proteins that are expressed in various tissues. Currently, 13 subtypes of AQPs (AQP0–AQP12) have been identified in mammals (King L S, et al., 2004). The distal small intestine and proximal colon are the major sites of AQP1, -3, -4, and -8 expression, suggesting that these proteins play an important role in cell function and fluid homeostasis. Yamamoto et al. reported that AQP4 and -8 expression levels in the colon were downregulated in mice with severe diarrhea following the experimental induction of food allergies (Yamamoto T, et al., 2007). Guttman et al. demonstrated that alterations in AQP2 and -3 localization might contribute to diarrhea in a mouse model following bacterial infection (Guttman J A, et al., 2007).

AQP3 reportedly played a critical role in the laxative effects of magnesium sulfate and bisacodyl by regulating fecal water content in the colon (Ikarashi N, Ushiki T, et al., 2011; Ikarashi N, et al., 2011). Our previous study found that decreased AQP1 mRNA expression inhibited water transfer from the intestinal tract to the vascular side, which eventually led to the development of diarrhea (Chen H, et al., 2009). Based on these results, this study was conducted to investigate the protein expression levels of AQP1, -3, -4, and -8 and pathological changes in intestine in jejunum, ileum, and colon in a mice model subjected to rotavirus-induced diarrhea.

MATERIALS AND METHODS

Cell and rotavirus culture

Rhesus monkey kidney (LLC-MK$_2$) cells were cultured in 1640 medium supplemented with 10% fetal bovine serum (Invitrogen, Carlsbad, CA, USA), 200 U/mL penicillin, and 200 μg/mL streptomycin at 37ºC and 5% CO_2.

Confluent monolayers of LLC-MK$_2$ cells were grown in 75-cm^2 flasks, washed 3 times with phosphate buffered saline (PBS), and 375 μL of rotavirus strain SA11 was added to the LLC-MK$_2$ cells. To induce propagation, rotavirus strain SA11 was activated with trypsin (10 μg/mL in medium) for 1 hour at 37ºC. After 1 hour of adsorption, the cells were washed 3 times with PBS and incubated in serum-free medium containing 1 μg/mL trypsin. Cells and medium were harvested when 100% cytopathological effects (CPE) were observed.

The infected LLC-MK$_2$ cells were disrupted by 3 cycles of freezing/thawing, and the cultured fluids were centrifuged for 30 minutes at 8000 rpm at 4ºC. Then the absorption of the final suspension was measured.

Viral infection was assayed in 96-well culture plates containing a confluent monolayer of LLC-MK$_2$ cells. After the growth medium was removed, each well was washed 3 times with PBS. Each well was inoculated with 100 μL of the virus, which had been serially diluted 10-fold. After adsorption for 1 hour at 37ºC, serum-free medium was added. The cultures were placed in the incubator at 37ºC. CPEs were observed every day. Five days after infection, 50% cell culture infective dose (CCID$_{50}$) was calculated according to the protocol described by Reed and Muench (Krah D L, et al., 1991), which was determined to be 1×10^7 CCID$_{50}$/mL.

Animal preparation and rotavirus enteritis model

All animal procedures were reviewed and approved by Guangzhou Women and Children's Medical Center Institutional Review Committee on Laboratory Animal Care, and all animals were handled in accordance with institutional guidelines. Three-day-old Kunming mice were obtained from Sun Yat-Sen University (Guangzhou, China). The experiment group consisted of 35 mice, which were administered 3 inoculations of 100 μL rotavirus strain SA11 via intragastric feeding tube every 2 hours. The control group consisted of 35 mice, which were administered 3 inoculations of 100 μL of uninfected LLC-MK$_2$ cells. Diarrhea was assessed by visually monitoring mice for up to 24 hours following intragastric challenge. A scoring system was used to determine the presence of diarrhea: 0, no stool; 1, brown formed stool; 2, brown soft stool; 3, yellow soft stool; and 4, yellow watery stool. If the score was $\geqslant 2$ points, the mice were diagnosed with diarrhea.

Detection of rotavirus antigen

The presence of the rotavirus antigen was tested using the rapid Rotavirus Test Kit (Colloidal Gold, Beijing, China). Fifty mg of formed stool or 100 μL watery stool was added to 0.5 mL of the extraction solution provided with the test kit. This combination was then stirred to homogenize. The results were read 15 minutes after incubation at room temperature. All procedures were conducted according to the manufacturer's instructions.

Sample collection and processing

Ileum specimens were obtained at necropsy from mice at 3 days postinfection and used for histopathological analysis. Specimens were fixed in buffered 10% formalin, routinely processed, embedded in paraffin, sectioned at 4 μm, stained with hematoxylin and eosin (HE), and examined using light microscopy. For electron microscopic examination, specimens were fixed in 3% neutral phosphate-buffered glutaraldehyde, postfixed in osmium tetroxide, dehydrated in graded ethanol, infiltrated with propylene oxide, and embedded in epoxy resin. Semithin (1 μm) sections were cut and stained with toluidine blue. Ultrathin (50–70 nm) sections were stained with uranyl acetate and lead citrate.

Two-cm-thick specimens were obtained from the jejunum, ileum, and colon, flushed with ice-cold saline, and frozen at -80ºC in liquid nitrogen for Western blot analysis.

Western blot analysis

Frozen tissue samples were sectioned into small pieces, homogenized, and dissolved for 30 minutes on ice in lysis buffer containing 20 mmol/L Tris (pH 7.4), 10% sucrose, 2 mmol/L EDTA-Na$_2$, 50 mmol/L NaF, 1% TritonX-100, and 0.1% sodium dodecyl sulfate. The mixture was sonicated before centrifugation at 12,000 rpm for 15 minutes at 4ºC to remove tissue debris. The supernatant was recentrifuged at 12,000 rpm for 10 minutes at 4ºC to obtain the membrane proteins. The membrane protein concentration was measured using the bicinchoninic acid (BCA) assay (Beyotime Biotech

Inc., Jiangsu, China). Equal amounts of total protein (50 µg) from each sample were loaded and separated using 10% sodium dodecyl sulfate polyacrylamide gel electrophoresis, then transferred to polyvinylidene difluoride membrane. Subsequently, the membranes were blocked with 5% milk containing TBS and 0.05% Tween-20 for 1 hour at room temperature, followed by overnight incubation at 4°C with either AQP1 (1:1000 rabbit polyclonal; ab125041; Abcam Inc., Cambridge, MA, UK), AQP3 (1:2000 rabbit polyclonal; ab153694; Abcam Inc., Cambridge, MA, UK), AQP4 (1:1000 rabbit polyclonal; sc-20812; Santa Cruz, CA, USA), or AQP8 antibodies (1:1000 rabbit polyclonal; ab15124; Abcam Inc., Cambridge, MA, UK). After washing 3 times with TBS-T, 1:10,000-diluted horseradish peroxidase (HRP) -conjugated anti-rabbit antibodies (ab6721; Abcam Inc., Cambridge, MA, UK) were incubated for 1 hour at room temperature. The target protein was detected using enhanced chemiluminescence Western blot detection reagents. Parallel Western blot analysis was performed using the anti-Glyceraldehyde 3-phosphate dehydrogenase (GADPH) monoclonal antibody (ab9385; Abcam Inc., Cambridge, MA, UK) as the loading control. Signals were detected using ECL Western Blot Detection Reagents (GE Healthcare, Buckinghamshire, UK) and exposed on X-ray film.

For the quantitative Western blot analysis, band intensities were quantified using an Odyssey scanner (LI-COR Biosciences; Lincoln, NE) and analyzed using ImageJ software (LI-COR, Lincoln, USA). Samples were prepared from 7 sets of nontreated and rotavirus strain SA11-treated mice. To minimize interference with data due to stage aberrations, sample preparation and statistical analyses were performed as follows: (1) 5 mice from each set were selected from the littermates; (2) signal intensities obtained from a single sample were expressed as a percentage of the summed signal intensities, which were obtained from 5 mice in the same set; and (3) this value was used to calculate the average and SD values for each set.

Statistical analyses

Data were expressed as means ± SDs. Differences between mean values were assessed using the unpaired student t test, and $p < 0.05$ was considered statistically significant.

RESULTS

Clinical symptoms and gross appearance of the intestinal tissues at necropsy

Mice were exposed to repeated oral SA11 virus challenges, which resulted in diarrhea within 24-hours postinfection and peaked within 3–4 days. Eight of 35 mice developed anorexia, 6 of 35 mice developed dehydration, and 12 of 35 mice developed abdominal distention. Fourteen of 35 mice developed frequent watery stools. Four mice became lethargic within 3–4 days postinfection, but the rest of the mice remained active and continued to drink breast milk throughout the study. Mice in the rotavirus-infected group did not gain weight. The nontreated normal mice developed no symptoms, and their weight increased by 0.2 g/day.

At necropsy, mild hyperemia in the jejunum and ileum were observed in mice that were administered the SA11 rotavirus. Diarrheic mice had watery yellow-white, yellow-brown, or brown-green colonic contents with flecks of undigested curd. There were no gross lesions in the control group.

Histopathology

The jejunum and ileum from the SA11 rotavirus-infected mice demonstrated patchy hyperemia. The microscopic findings were characterized by mild multifocal villus atrophy and necrosis, scattered hyperplastic crypts, and occasional goblet cell-filled crypts. Mild inflammatory cell infiltrates were occasionally scattered within the lamina propria. The intestinal mucosa was normal in the control group (Figure 1A). While the submucosa demonstrated variable edema, the blood vessels were occasionally dilated and ileal epithelial cells demonstrated vacuolar degeneration in SA11-infected mice (Figure 1B).

Ultrastructure of the ileal tissue

Electron microscopy was used to examine the ultrastructure. Ileal specimens were obtained from select SA11 rotavirus-infected mice at 3 days postinfection demonstrated adipose particles, vacuoles in the villus enterocytes, and occasional goblet cells. Infected enterocytes demonstrated intracytoplasmic lipid globules, malaligned or defluxed microvilli, increases in the number of lysosomes, mitochondrial swelling, and dilated endoplasmic reticulum, but no obvious structural changes were noted at the cell junctions (Figure 2).

AQP protein expressions

AQP1, AQP3, AQP4, and AQP8 protein expression levels were determined in the nontreated normal mice and SA11 rotavirus-treated mice using Western blot analysis (Figure 3). There were no significant differences in any AQPs in the jejunum between groups. AQP1 expression was significantly reduced in the ileum and colon of mice after SA11 virus exposure in comparison with nontreated normal mice ($p < 0.05$ for the ileum; $p < 0.01$ for the colon) (Figure 3A). Likewise, AQP4 (Figure 3B) and AQP8 protein expression levels (Figure 3C) were significantly attenuated in the colon of SA11 virus-infected mice ($p < 0.01$ for AQP4; $p < 0.05$ for AQP8). However,
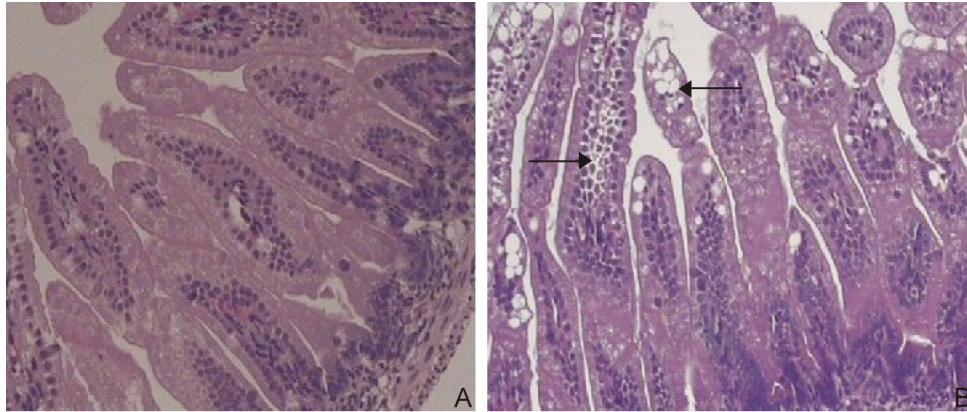
Figure 1. HE-stained ileal mucosa in mice infected with rotavirus strain SA11. A: The ileal mucosa appears normal in the control mice. B: In SA11-infected mice, the ileal epithelial cells show vacuolar degeneration (Magnification: 200×).
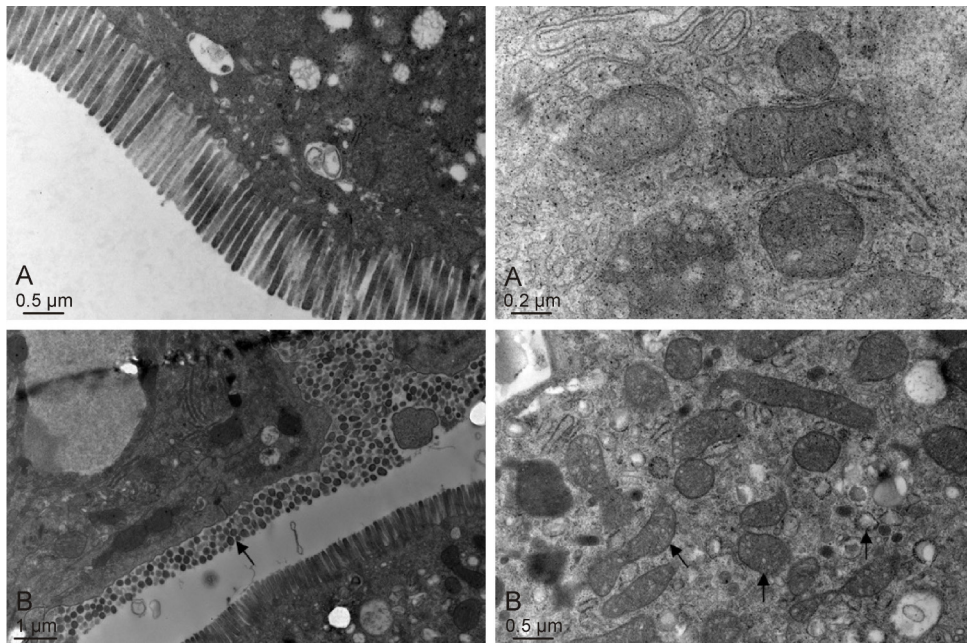

Figure 2. Ultrastructure of ileal specimens obtained from rotavirus strain SA11-infected mice. (A, upper left & right) The ultrastructure of the ileum is normal in control mice. (B, lower left & right) The rotavirus SA11-induced diarrheic mice show malaligned or defluxed microvilli, mitochondrial swelling, and an increase in the number of lysosomes.

AQP3 protein expression was significantly increased in the colon of the SA11 rotavirus-infected mice in comparison with the controls ($p < 0.01$) (Figure 3D).

DISCUSSION

Sheridan et al. was the first researcher to describe a mouse model of rotavirus infection in their study of virus-specific immunity (Sheridan J F, et al., 1983). The neonatal mice that received SA11 antigen-positive cells developed diarrhea that lasted $\geqslant 9$ days. Mice are considered a reliable animal model for studying immune responses during primary rotavirus infection (Knipping K, et al., 2011). In our mouse model of rotavirus diarrhea, mice developed profusely liquid stools 24 hours after exposure to SA11 strain. Microscopically, vacuolar degeneration, multifocal villus atrophy, and necrosis in the ileum were noted. Electronic microscopy revealed intra-
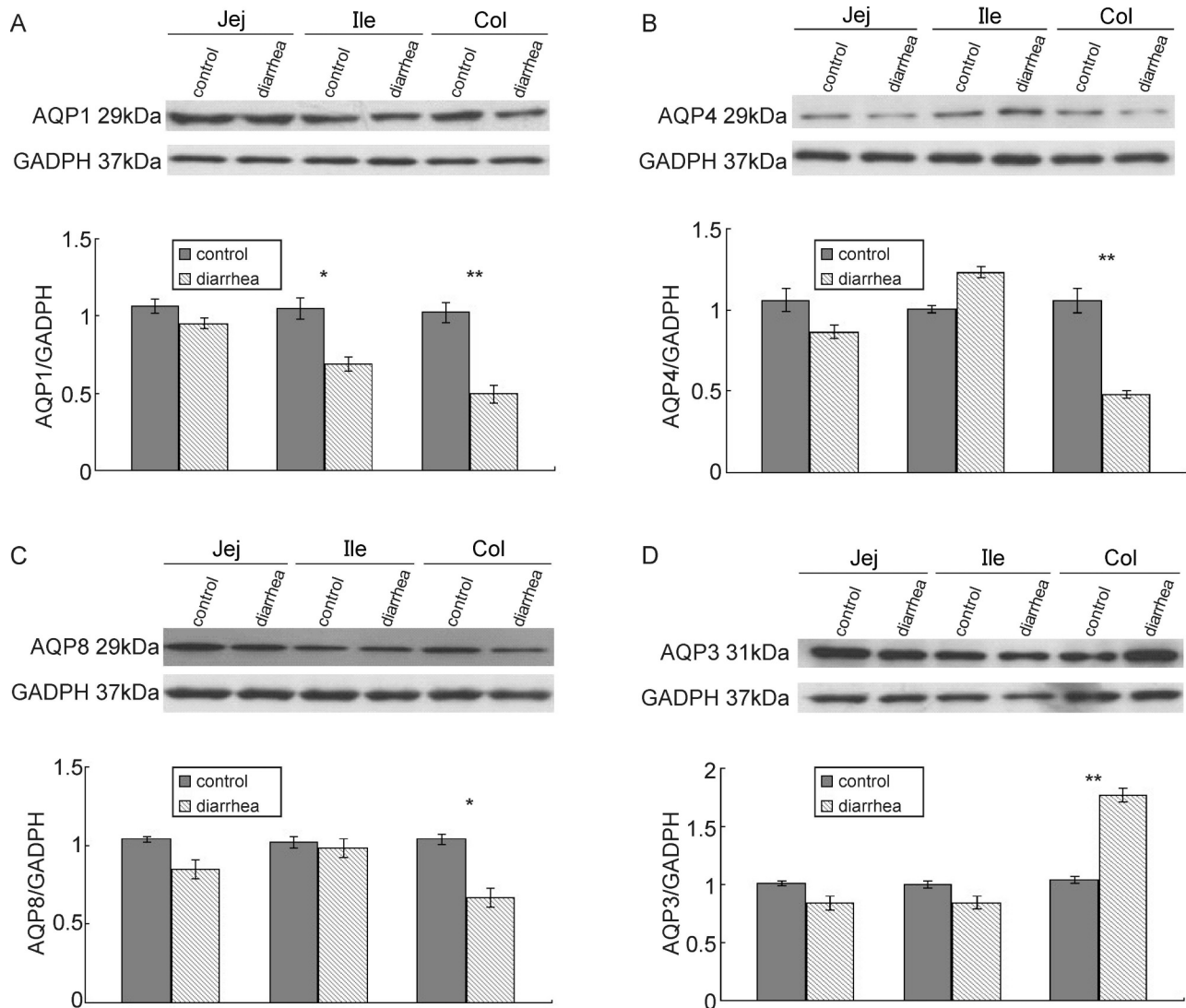
Figure 3. Western blots of AQPs in the intestines of rotavirus strain SA11-treated mice. In comparison with control animals, mice infected with SA11 demonstrated (A) decreased AQP1 protein levels in the ileum and colon, (B) decreased AQP4 levels, (C) decreased AQP8 levels in colon, and (D) increased AQP3 expression levels in the colon. Jej, jejunum; Ile, ileum; col, colon. *$p < 0.05$; **$p < 0.01$ in comparison with the control group.

cytoplasmic lipid globules, mitochondrial swelling, and endoplasmic reticulum dilatation. By establishing this animal model, we are able to investigate if altered AQP expression levels in the intestines are associated with the development of rotavirus diarrhea.

At least 7 AQP subtypes (AQPs 1, 3, 4, 5, 7, 8, 9, and 11) are reportedly expressed in the gastrointestinal tract and play important roles in several physiological and pathological processes. In particular, the colon is a major site for AQP1, 3, 4, and 8 expression (Yamamoto T, et al., 2007), and there is some evidence regarding the physiological roles and functions of AQP1, 3, 4, and 8. Chen et

al. (Chen H, et al., 2009) reported that AQP1 mRNA was significantly decreased after exposure to rotavirus SA11 in a mouse model of rotavirus-induced diarrhea. AQP1 protein expression demonstrates a similar pattern to that observed for AQP1 mRNA in our present research. AQP1 mRNA was upregulated in the traditional Chinese medicine antidiarrheal oral liquid treatment group, which further suggested that the decrease in AQP1 inhibited water transfer from the intestinal tract to the vascular side and caused diarrhea. However, there were no significant difference in AQP3, 4, and 8 expression between the rotavirus diarrhea group and treated with Chinese medi-

cine antidiarrheal oral liquid group. In our present study, the expression levels of AQP4 and AQP8 decreased while AQP3 increased. This difference might have been caused by the quantity of samples and diarrhea severity. Our results are consistent with those reported by other researchers (Yamamoto T, et al., 2007; Ikarashi N, et al., 2011; Wang K S, et al., 2000; Laforenza U, et al., 2005; Hardin J A, et al., 2004; Ma T, et al., 2001; Tsujikawa T, et al., 2003). AQP1 reportedly plays a major role in pancreatic secretion, bile concentration, and water reabsorption in colon. Ma T et al. demonstrate that AQP1 knockout mice develop steatorrhea and a blunted weight gain when fed a high-fat diet, suggesting that AQP1 deletion causes the defective secretion of fluid across cells in the biliary tract and pancreatic acini/ducts and alters the quantity and/or composition of secreted fluids (Ma T, et al., 2001). In streptozotocin-induced diabetic rats, the number of AQP1-immunoreactive neurons significantly increase, indicating that AQP1 plays an important role in diabetic gastrointestinal dysfunctions such as diarrhea and constipation (Ishihara E, et al., 2008). The water content of defecated stool is also higher in AQP4-knockout mice (Wang K S, et al., 2000), and inhibiting AQP8 expression by small interfering RNA significantly decreases water absorption in rat colon (Laforenza U, et al., 2005), indicating that AQP4 and AQP8 may play major roles in water movement through the colon by acting on the apical side of the superficial cells. In addition, allergic diarrhea is associated with the downregulation of AQP4 and AQP8 expression in the proximal colon of mice (Yamamoto T, et al., 2007). Interestingly, in a murine model of colitis and in patients with inflammatory bowel disease or infectious colitis, significant alterations in colonic fluid secretion are correlated with reduced AQP4 and AQP8 expression. Patients have also developed severe diarrhea and reduced AQP expression levels (Hardin J A, et al., 2004). These results are consistent with our findings that AQPs are reduced in mice with severe diarrhea due to the experimental administration of rotavirus.

We also found that the AQP1 protein expression levels in the ileum, and AQP1, AQP4, and AQP8 levels in the colon, were significantly attenuated in rotavirus-infected mice, suggesting that these AQPs contribute to decreased colonic water absorption and subsequently diarrhea.

AQP3 in the colon was also upregulated after SA11 infection. We speculate that this is a compensatory mechanism to avoid severe diarrhea and further dehydration. Tsujikawa et al. also found that among rats with 80% distal small bowel resection, AQP3 mRNA expression significantly increased in the residual small intestine and colon. Diarrhea gradually improved, most likely due to an adaptive response to increased water absorption (Tsujikawa T, et al., 2003). In addition, Ikarashi et al re-

ported that AQP3 protein expression in the colon significantly increases over time following the administration of osmotic laxative or magnesium sulfate-induced diarrhea (Ikarashi N, et al., 2011). Apparently, the compensatory increase in AQP3 found here was still insufficient to prevent diarrhea.

In conclusion, here we demonstrate that low AQP1 protein expression in the ileum and AQP1, AQP4, AQP8 protein expression in the colon play an important role in rotavirus diarrhea. Our work provides important insights into the mechanisms of rotavirus-induced diarrhea. Further analysis of the underlying molecular mechanisms that downregulate AQPs in the colon is required.

ACKNOWLEDGMENTS

COMPLIANCE WITH ETHICS GUIDELINES

All the authors declare that they have no competing interests. All animal procedures were reviewed and approved by Guangzhou Women and Children's Medical Center Institutional Review Committee on Laboratory Animal Care and all animals were handled in accordance with institutional guidelines.

AUTHOR CONTRIBUTIONS

Cao M W carried out the experiments, and drafted the article. Yang M, Chen H, Chen P Y, and Geng L L analyzed the data. Ou Z Y, Yang M, Li D Y and Gong S T involved in designing, drafting the manuscript and revising it critically for important intellectual content. All authors read and approved the final manuscript.

REFERENCES

Centers for Disease Control and Prevention (CDC). 2008. Rotavirus surveillance--worldwide, 2001–2008. MMWR Morb Mortal Wkly Rep, 57: 1255–1257.

Chen H, Gong S T, Ou W J. 2009. Expression of Aquaporins in Rotavirus Enteritis Treatment by Drug. Progr Modern Biomed. 17: 3258–3261. (In Chinese)

Guttman J A, Samji F N, Li Y, Deng W, Lin A, Finlay B B. 2007. Aquaporins contribute to diarrhoea caused by attaching and effacing bacterial pathogens. Cell Microbiol, 9: 131–141.

Hardin J A, Wallace L E, Wong J F, O'Loughlin E V, Urbanski S J, Gall D G. 2004. Aquaporin expression is downregulated in a murine model of colitis and in patients with ulcerative colitis, Crohn's disease and infectious colitis. Cell Tissue Res, 318: 313–323.

Hodges K, Gill R. 2010. Infectious diarrhea: Cellular and molecular mechanisms. Gut Microbes, 1: 4–21.

Ikarashi N, Baba K, Ushiki T, Kon R, Mimura A, Toda T. 2011. The laxative effect of bisacodyl is attributable to decreased aquaporin-3 expression in the colon induced by increased PGE2 secretion from macrophages. Am J Physiol Gastrointest Liver Physiol, 301: G887–G895.

Ikarashi N, Ushiki T, Mochizuki T, Toda T, Kudo T, Baba K. 2011. Effects of magnesium sulphate administration on aquaporin 3 in rat gastrointestinal tract. Biol Pharm Bull, 34: 238–242.

Ishihara E, Nagahama M, Naruse S, Semba R, Miura T, Usami M. 2008. Neuropathological alteration of aquaporin 1 immunoreactive enteric neurons in the streptozotocin-induced diabetic rats. Auton Neurosci, 138: 31–40.

King L S, Kozono D, Agre P. 2004. From structure to disease: the evolving tale of aquaporin biology. Nat Rev Mol Cell Biol, 5: 687–698.

Knipping K, McNeal M M, Crienen A, van Amerongen G, Garssen J, Van't Land B. 2011. A gastrointestinal rotavirus infection mouse model for immune modulation studies. Virol J, 8: 109.

Krah D L. 1991. A simplified multiwell plate assay for the measurement of hepatitis A virus infectivity. Biologicals, 19: 223–227.

Laforenza U, Cova E, Gastaldi G, Tritto S, Grazioli M, LaRusso N

F. 2005. Aquaporin-8 is involved in water transport in isolated superficial colonocytes from rat proximal colon. J Nutr, 135: 2329–2336.

Ma T, Jayaraman S, Wang K S, Song Y, Yang B, Li J . 2001. Defective dietary fat processing in transgenic mice lacking aquaporin-1 water channels. Am J Physiol Cell Physiol, 280: C126–C134.

Sheridan J F, Eydelloth R S, Vonderfecht S L, Aurelian L. 1983. Virus-specific immunity in neonatal and adult mouse rotavirus infection. Infect Immun, 39:917–927.

Tsujikawa T, Itoh A, Fukunaga T, Satoh J, Yasuoka T, Fujiyama Y. 2003. Alteration of aquaporin mRNA expression after small bowel resection in the rat residual ileum and colon. J Gastroenterol Hepatol, 18: 803–808.

Wang K S, Ma T, Filiz F, Verkman A S, Bastidas J A. 2000. Colon water transport in transgenic mice lacking aquaporin-4 water channels. Am J Physiol Gastrointest Liver Physiol, 279: G463–G470.

Yamamoto T, Kuramoto H, Kadowaki M. 2007. Downregulation in aquaporin 4 and aquaporin 8 expression of the colon associated with the induction of allergic diarrhea in a mouse model of food allergy. Life Sci, 81: 115–120.